



Research Paper

Autocrine IL-10 functions as a rheostat for M1 macrophage glycolytic commitment by tuning nitric oxide production [☆], [☆] [☆]



Walter A. Baseler ^a, Luke C. Davies ^{a,b}, Laura Quigley ^a, Lisa A. Ridnour ^a, Jonathan M. Weiss ^a, S. Perwez Hussain ^c, David A. Wink ^a, Daniel W. McVicar ^{a,*}

^a Cancer and Inflammation Program, Center for Cancer Research, National Cancer Institute, Frederick, MD 21702, United States

^b Division of Infection and Immunity, School of Medicine, Cardiff University, Cardiff, UK

^c Laboratory of Human Carcinogenesis, Center for Cancer Research, National Cancer Institute, Bethesda, MD 20892, United States

ARTICLE INFO

Article history:

Received 22 July 2016

Received in revised form

13 September 2016

Accepted 14 September 2016

Available online 16 September 2016

ABSTRACT

Inflammatory maturation of M1 macrophages by proinflammatory stimuli such as toll like receptor ligands results in profound metabolic reprogramming resulting in commitment to aerobic glycolysis as evidenced by repression of mitochondrial oxidative phosphorylation (OXPHOS) and enhanced glucose utilization. In contrast, “alternatively activated” macrophages adopt a metabolic program dominated by fatty acid-fueled OXPHOS. Despite the known importance of these developmental stages on the qualitative aspects of an inflammatory response, relatively little is known regarding the regulation of these metabolic adjustments. Here we provide evidence that the immunosuppressive cytokine IL-10 defines a metabolic regulatory loop. Our data show for the first time that lipopolysaccharide (LPS)-induced glycolytic flux controls IL-10-production via regulation of mammalian target of rapamycin (mTOR) and that autocrine IL-10 in turn regulates macrophage nitric oxide (NO) production. Genetic and pharmacological manipulation of IL-10 and nitric oxide (NO) establish that metabolically regulated autocrine IL-10 controls glycolytic commitment by limiting NO-mediated suppression of OXPHOS. Together these data support a model where autocrine IL-10 production is controlled by glycolytic flux in turn regulating glycolytic commitment by preserving OXPHOS via suppression of NO. We propose that this IL-10-driven metabolic rheostat maintains metabolic equilibrium during M1 macrophage differentiation and that perturbation of this regulatory loop, either directly by exogenous cellular sources of IL-10 or indirectly via limitations in glucose availability, skews the cellular metabolic program altering the balance between inflammatory and immunosuppressive phenotypes.

© 2016 Published by Elsevier B.V. This is an open access article under the CC BY-NC-ND license (<http://creativecommons.org/licenses/by-nc-nd/4.0/>).

1. Introduction

Macrophages are an integral part of the innate immune system; critical in the maintenance of tissue homeostasis in the healthy state and instrumental in orchestrating inflammatory responses during disease [1]. Tissue macrophages at homeostasis or those exposed to cytokines associated with Th2- responses (e.g. IL-4/13) are considered anti-inflammatory. These cells, termed “M2 or “alternatively activated”, produce the cytokine interleukin-10 and are characterized via enhanced expression of arginase-1, and

scavenger receptors such as SR-A and MARCO. In contrast, “classically activated” or “M1” macrophages are the result of bacterial/toll-like receptor (TLR) engagement in conjunction with cytokines associated with a Th1-like response (e.g. Interferon gamma). These cells are highly inflammatory, producing pro-inflammatory cytokines such as IL-12 and tumor necrosis factor (TNF), as well as inflammatory intermediates including eicosanoids, reactive oxygen and nitrogen species [2]. Consistent with their role in the regulation of inflammatory responses, skewing the development, expansion or perseverance of macrophages through genetic or biochemical means can result in profound effects for diseases including rheumatoid arthritis.

Regardless of their activation status, macrophages must balance their metabolic demands for energy with the needs of biosynthetic pathways necessary for a particular functional profile. For example, classically activated inflammatory macrophages must simultaneously produce abundant inflammatory cytokines and

^{☆☆}This work was funded in part by the Intramural Research Program of the National Cancer Institute. LCD is funded in part by the Wellcome Trust, UK.

[†]The content of this publication does not reflect views or policies of the Department of Health and Human Services, nor does mention of trade names, commercial products, or organizations imply endorsement by the U.S. Government.

* Corresponding author.

E-mail address: mcvicard@mail.nih.gov (D.W. McVicar).

lipids, while generating the ATP and NADPH necessary for a robust oxidative burst needed for pathogen killing. In addition, they generate the energy needed for cell adhesion and motility, and the anabolic intermediates used in the nucleotide synthesis necessary for enhanced gene expression and proliferation [3]. Lastly, recent evidence suggests that in dendritic cells, mitochondrial citrate export during stimulation supports production of cytosolic acetyl-CoA critical for lipid synthesis that facilitates expansion of Golgi and endoplasmic reticulum needed for effective production of inflammatory cytokines. Only when each of these demands is met can a macrophage effectively carry out its function.

To satiate immediate metabolic demands it would seem intuitive for activated leukocytes to utilize aerobic glycolysis, a quick but inefficient mechanism for producing ATP. Indeed, recent literature has suggested that both macrophages and dendritic cells (DC) undergo a metabolic shift away from mitochondrial oxidative phosphorylation (OXPHOS) towards aerobic glycolysis when stimulated with the gram-negative bacterial component lipopolysaccharide (LPS), a process that has been termed “glycolytic commitment” [4,5]. The profound shift in metabolism permits leukocytes to generate the requisite energy for functionality while producing the glycolytic intermediates necessary for the pentose phosphate pathway (PPP) critical for growth and maintenance of redox potential. As a result, “classically activated” M1 macrophages that are pro-inflammatory are largely dependent on aerobic glycolysis and exhibit low levels of mitochondrial respiration [4,6]. Conversely, macrophages “alternatively activated” with IL-4 are not glycolytically committed and instead utilize mitochondrial fatty acid oxidation (FAO) for energy production [7,8].

Though commitment to aerobic glycolysis upon leukocyte activation has been well documented, the mechanisms associated with the metabolic reprogramming of macrophages remain poorly defined. Tannahill et al. recently suggested that macrophage glycolytic commitment is, in part, due to an LPS-induced “pseudo hypoxic” state in which high succinate promotes stabilization of HIF-1 α , resulting in enhanced glycolysis via expression of glycolytic genes [4]. In parallel, HIF-1 α promotes expression of pyruvate dehydrogenase kinase 1, an inhibitor of pyruvate dehydrogenase, effectively blocking acetyl-CoA entry into the tricarboxylic acid (TCA) cycle [9,10]. In contrast, Everts et al. has implicated nitric oxide (NO) production in LPS-stimulated DC as the driving force in OXPHOS repression via direct inhibition of the mitochondrial electron transport chain (ETC). It remains unknown if this mechanism plays a role in macrophage metabolism [11].

Interleukin-10 is a potent immunoregulatory cytokine due to its ability to suppress inflammatory responses and induce development of T regulatory cells. In the metabolic context, TLR-directed DC glycolytic reprogramming and subsequent inflammatory responses are blunted via addition of IL-10 [12]. In contrast to DC, stimulated macrophages are capable of producing relatively high levels of IL-10 suggesting this cytokine might participate in autocrine and paracrine control of metabolic programming. Using biochemical approaches, gene targeted mice, and metabolic flux analysis, and unbiased metabolomics analysis, here we show that LPS-driven IL-10 production functions as a metabolic rheostat in macrophages, permitting these cells to maintain metabolic equilibrium.

2. Materials and methods

2.1. Reagents and antibodies

DETA/NO, PAM₃CSK₄, LPS (*Escherichia coli* 0111:B4), 2-Deoxy-D-glucose (2-DG), oligomycin, rotenone and the mTOR inhibitor Rapamycin were from Sigma-Aldrich (St. Louis, MO). 2-(N-(7-

Nitrobenz-2-oxa-1,3-diazol-4-yl)Amino)-2-Deoxyglucose (2-NBDG) was purchased through Life Technologies (Grand Island, NY). Western blotting antibodies anti-AMPK α (#2603) and anti-phospho-AMPK α (phospho Thr172) (#2535) were from Cell Signaling Technology (Beverly, MA). Anti-phospho-mTOR (phospho S2481) (#ab137133) antibody was from Abcam (Cambridge, MA). Anti-Actin (MAB1501) antibody was from Chemicon International (Temecula, CA). Human and mouse Enzyme-Linked Immunosorbent Assay (ELISA, IL-10 and TNF α) kits were purchased through eBioscience (San Diego, CA) and experimentation was performed per manufacturer's protocol.

2.2. Mice

Il10^{-/-} and C57BL/6 control mice were maintained and bred in the Frederick National Laboratory Core Breeding Facility. Animal care was provided in accordance with the procedures in, “A Guide for the Care and Use of Laboratory Animals”. Ethical approval for the animal experiments detailed in this manuscript was received from the Institutional Animal Care and Use Committee (Permit Number: 000386) at the NCI-Frederick.

2.3. Macrophage culture, stimulation, and immunoblotting

Mouse bone marrow derived macrophages (BMDM) [13] and human monocyte-derived macrophages (MDM) [14] were isolated and cultured as previously described. After growing BMDM or human MDM for 6 days in culture, cells were placed in complete culture media and pretreated with 2 or 5 mM 2-deoxyglucose (2-DG) or 100 nM rapamycin for 30 min as indicated prior to addition of 100 ng/mL of LPS for 4–24 h. For glucose deprivation studies, cultured BMDM were incubated in culture media containing decreasing glucose for 30 min prior to addition of 100 ng/mL of LPS for 4 h. Protein expression in stimulated macrophages was determined by western blot as previously described [15]. Due to the protein size similarities, AMPK and pAMPK were analyzed on parallel blots.

2.4. Metabolic analyses

Oxygen consumption rate (OCR) and extracellular acidification rate (ECAR) were examined using the XF24 Seahorse Metabolic Analyzer from Seahorse Biosciences. Briefly, cultured BMDM were plated at a seeding density of 3×10^5 cells/well in 500 μ l of complete media. Where noted, data are represented as percent of control levels calculated as the mean of the third set of flux readings. All additional values for a given sample are reported relative to this. Metabolic mitochondrial stress tests were performed via manufacturer's protocol. Mitochondrial OCR is defined as the percentage of OCR that is oligomycin sensitive. OCR/ECAR ratios were calculated using the first nine determinations of basal OCR and basal ECAR where indicated. When indicated, 100 ng/mL LPS, 10 mM 2-DG, and/or 1 μ M DETA/NO was added during the assay to assess metabolic changes. In other assays, BMDM were incubated in complete culture media supplemented with 100 ng/mL of LPS overnight. Total cellular ATP was assessed using The ATP Determination Kit (Invitrogen) as per the manufacturer's directions. Glucose uptake was assayed in BMDM using fluorescent glucose analog 2-(N-(7-Nitrobenz-2-oxa-1,3-diazol-4-yl)Amino)-2-Deoxyglucose (2-NBDG) per manufacturer's protocol. Fluorescent uptake was analyzed using LSRFortessa flow cytometer (BD Biosciences). Data were analyzed using Flowjo software. NO activity was assessed via the Greiss Reagent System (Promega), which measures nitrite concentrations.

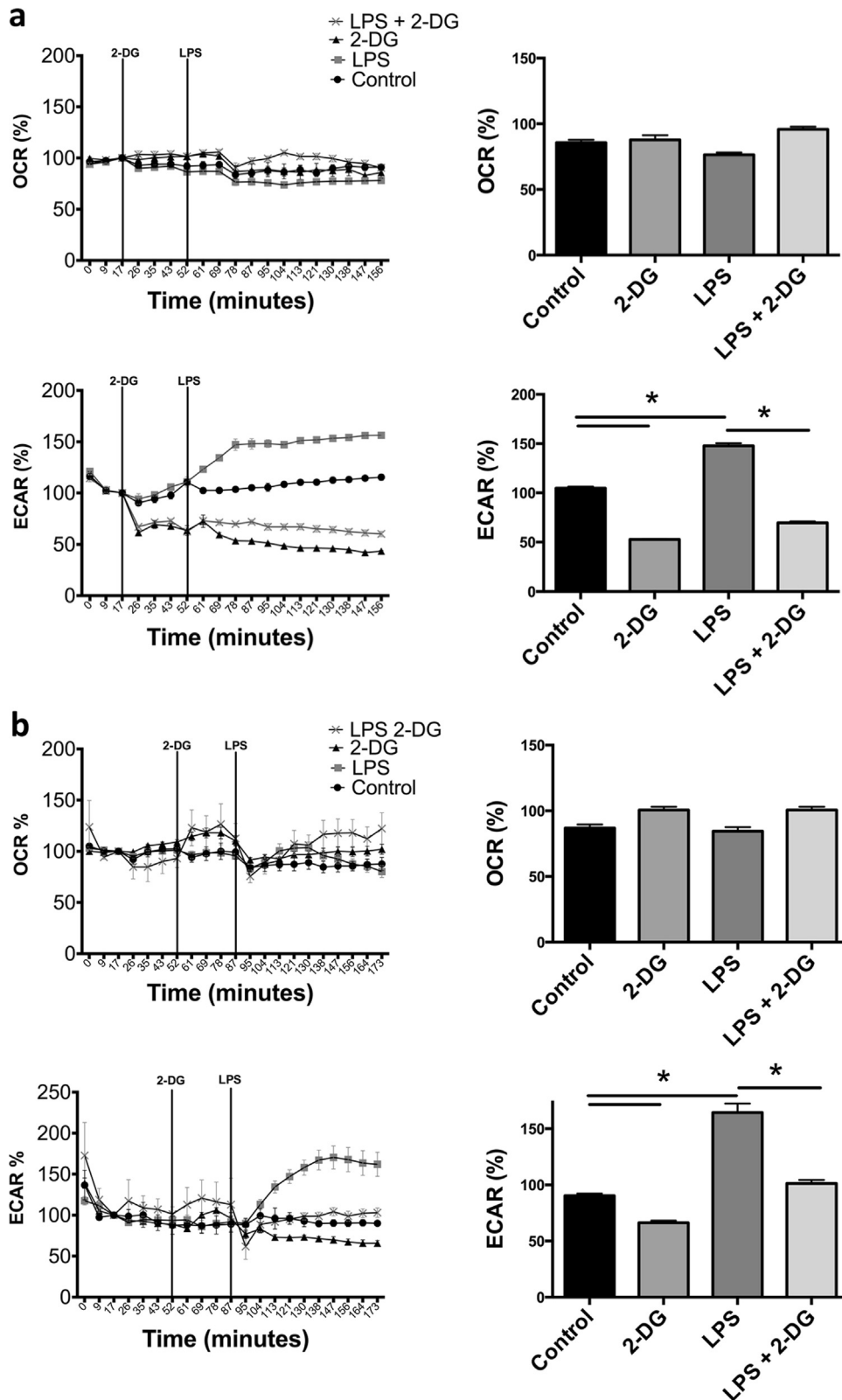


Fig. 1. Acute LPS stimulation of human and mouse macrophages leads to an immediate glycolytic burst that is dependent on glucose. Real time OCR and ECAR percent changes in mouse BMDM \pm 5 mM 2-DG and 100 ng/mL LPS or a combination of both (a). Human MDM real time OCR and ECAR stimulated \pm 10 mM 2-DG, 100 ng/mL of LPS or a combination of both (b). Data represent percent of resting control levels and are from one experiment representative of 2 (b) or 3 (a) independent experiments (mean \pm standard error of the mean (SEM) of the final three time points, $n=5$ per group). Values for bar graphs are derived from the three data points following addition of the experimental agent as noted on the line graphs. * $p < 0.05$. Statistical significance was assessed by ANOVA with a Bonferroni post-test.

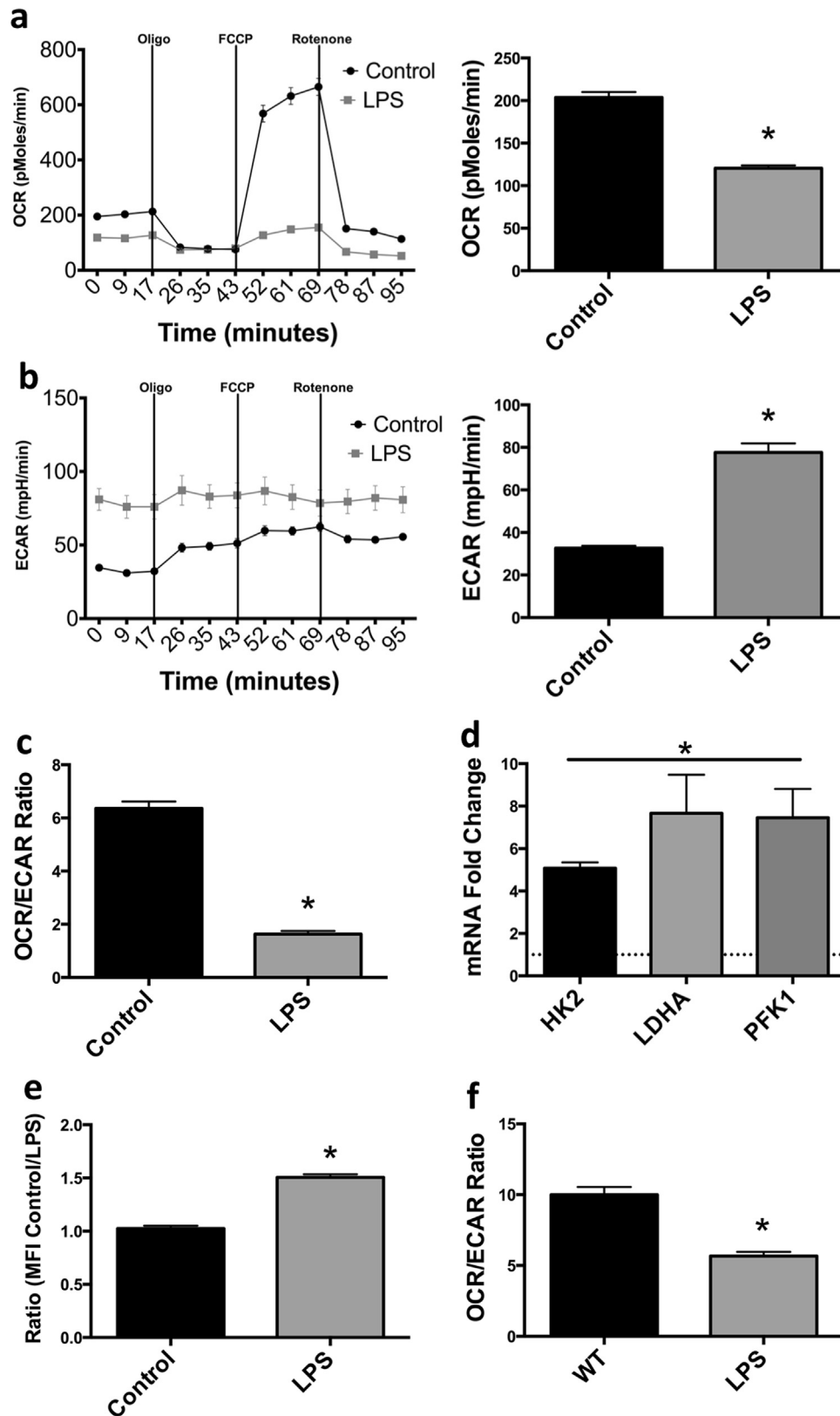


Fig. 2. Prolonged stimulation of macrophages with LPS leads to glycolytic commitment. OCR, ECAR and OCR/ECAR ratio of mouse BMDM 24 h after LPS administration (100 ng/mL) (a–c). mRNA levels of glycolytic enzymes HK2, LDHA, and PFK1 were evaluated 24 h after LPS administration to BMDM in which the dotted line indicates control levels (d). Glucose uptake in LPS treated macrophages (24 h) was assessed by fluorescent 2-NBDG (100 μ M) uptake via flow cytometry (e). OCR/ECAR ratio was evaluated in human MDM 24 h after exposure to 100 ng/mL LPS (f). Metabolic data (a–c, f) are from one experiment representative of at least 3 independent experiments (mean \pm SEM $n=5$). mRNA analysis (d) is a combination of 2 independent experiments ($N=5$). 2-NBDG analysis (e) is a combination of 3 independent experiments * $p < 0.05$. Statistical significance was assessed by Student's t test.

2.5. Primary metabolomic analysis

Wild type (WT) and *Il10*^{-/-} BMDM (~10 million cells) were treated with vehicle (PBS) or 100 ng/mL of LPS for 24 h. Cells were then washed, gently scraped, pelleted, snap frozen in liquid nitrogen and sent to West Coast Metabolomic Center at the University of California, Davis for metabolomic analyses. Briefly, samples were extracted by 1 mL of degassed acetonitrile, isopropanol and water in proportions 3:3:2 at -20 °C, centrifuged and decanted to complete dryness. A clean-up step with acetonitrile/water (1:1) removes membrane lipids and triglycerides. The cleaned extract is aliquoted into two equal portions and the supernatant is dried down again. Internal standards C08–C30 FAMES are added and the sample is derivatized by methoxyamine hydrochloride in pyridine and subsequently by N-methyl-N-trimethylsilyltrifluoroacetamide for trimethylsilylation of acidic protons. Gas Chromatography-Time of Flight analysis was performed by Agilent GC6890/LECO Pegasus III MS.

2.6. Statistical analysis

Data are presented as means ± standard error of mean (± SEM) and are representative of at least 2 independent experiments. One-way ANOVA followed by Bonferroni's post was used for statistical analysis when multiple groups were analyzed. Student *t* test or Mann-Whitney test were used for statistical analysis when two groups were analyzed. Statistical significance was set at **p* < 0.05.

3. Results

3.1. Resting macrophages utilize distinct metabolites to fuel OXPHOS and aerobic glycolysis

Macrophages have the ability to metabolize glucose, fatty acids, and glutamine to fuel both aerobic glycolysis and OXPHOS [3]. Consistent with previous literature, we found BMDM to have substantial oxygen consumption rates (OCR) and low extracellular acidification rates (ECAR) resulting in substantial OCR/ECAR ratios (Fig S1A). Further, BMDM OCR was fueled predominantly via fatty acid oxidation (FAO) and ECAR fueled via glucose (Fig S1B and E). Interestingly, oligomycin caused a suppression of OCR and a reactive increase in ECAR, possibly in an effort to maintain metabolic homeostasis (Fig S1). Together these results demonstrate that resting BMDM are plastic metabolically but preferentially generate ATP via the utilization of FAO.

3.2. LPS stimulated mouse BMDM and human macrophages undergo glycolytic reprogramming

Having established the basal metabolic status of macrophages we next analyzed metabolic responses of BMDM to LPS. LPS stimulation resulted in a progressive increase in ECARs within minutes (Fig. 1A). OCRs were unaffected over this timeframe (Fig. 1A). As shown in Fig. 1, addition of 2-DG during bioenergetic monitoring leads to an instant repression of basal ECARs. Further, 2-DG severely blunts LPS-stimulated increases in ECAR indicating glucose is absolutely necessary for the acute glycolytic elevation in BMDM. Identical results were found using human monocyte-derived macrophages (MDM) stimulated with LPS in the presence or absence of 2-DG (Fig. 1B). Together these data confirm that 2-DG inhibits the immediate LPS-induced increase in glycolytic flux.

In contrast, prolonged stimulation (24 h) of BMDM with LPS leads to a glycolytic phenotype characterized by enhancement of ECAR in combination with significant reductions to OCR (Fig. 2A

and B). Best quantitated by a decline in OCR/ECAR ratios; this state has been termed “glycolytic commitment” in inflammatory DC [11] (Fig. 2C). Notably, the reduction in OXPHOS due to LPS affects both basal OCR levels as well as spare respiratory capacity indicating a global suppression of OXPHOS. As expected, glycolytic commitment was associated with transcriptional metabolic reprogramming. BMDM stimulated with LPS for 24 h display significant increases to multiple glycolytic genes including hexokinase-2 (*Hk2*), lactate dehydrogenase A (*Ldha*) and phosphofructokinase 1 (*Pfk1*) (Fig. 2D). LPS-treated BMDM import ~50% more glucose than unstimulated controls as measured with the fluorescent glucose analog 2-NBDG (Fig. 2E). Notably, as shown in Fig. 2F, human MDM also undergo a strong glycolytic commitment as evidenced by a reduction in OCR/ECAR ratios after overnight culture with LPS. Taken together, these results show that endotoxin stimulated BMDM undergo an immediate increase in aerobic glycolysis followed by a sustained glycolytic commitment associated with transcriptional modification of metabolic genes.

3.3. Inhibition of LPS-driven glycolysis reduces IL-10 production

Given that macrophages preferentially utilize glycolysis upon endotoxin stimulation, we sought to determine the ramifications of interference of LPS-induced glycolysis via blockade of glucose utilization with 2-DG might have on inflammatory outcome. We assayed levels of the LPS-inducible cytokines TNFα and IL-10. Interestingly, quantitative RT-PCR analyses revealed a substantial reduction in *Il10* mRNA and a modest increase in *Tnfa* when BMDM were pretreated with 2-DG 30 min prior to a 4 h stimulation with LPS (Fig. 3A and B). 2-DG suppression of IL-10 production was confirmed by assaying secreted IL-10, with no significant change in secreted TNFα (Fig. 3C and D). To ensure these results were not off-target effects of 2-DG, BMDM were stimulated with LPS in decreasing amounts of glucose. BMDM stimulated in media with less than 0.5 mM glucose produced less IL-10 than those cultured in higher levels with no significant change in TNFα (Fig. 3E and F). Additionally, human MDM cultured under identical conditions mirrored the preferential reduction of IL-10 with 2-DG pre-stimulation (Fig. 3G and H). Together these data show that LPS-induced IL-10 production is sensitive to the availability of glucose in macrophages.

3.4. IL-10 production is regulated via AMPK sensing of cellular ATP levels

Mammalian target of rapamycin (mTOR) is a mediator of IL-10 production in macrophages, and is in turn regulated by AMP kinase (AMPK). AMPK is a metabolic sensor that detects elevations in ATP/AMP ratios within the cell and initiates programs to increase ATP production [16]. Therefore, we hypothesized that glucose deprivation of glycolytically committed macrophages might result in reductions in cellular ATP levels, activation of AMPK, repression of mTOR and reduced IL-10 production. To test this possibility, we stimulated macrophages with LPS in the presence or absence of 2-DG and assayed cellular ATP (Fig. 4A). In addition, we stimulated cells with LPS and 2-DG before western blotting to detect the levels of phosphorylated AMPK (pAMPK) and phosphorylated mTOR (pMTOR) (Fig. 4B). BMDM stimulated with LPS had lower levels of ATP but these levels were not sufficient to elicit the activation of AMPK. Rather, in LPS stimulated macrophages levels of pAMPK fell and mTORC activation proceeded unabated (Fig. 4B). In contrast, incubation of macrophages with 2-DG or 2-DG followed by LPS administration reduced ATP levels to lower than LPS treatment alone (Fig. 4A). Accordingly, BMDM treated with 2-DG or 2-DG and LPS now showed enhanced pAMPK and concomitant repression of mTOR activation consistent with

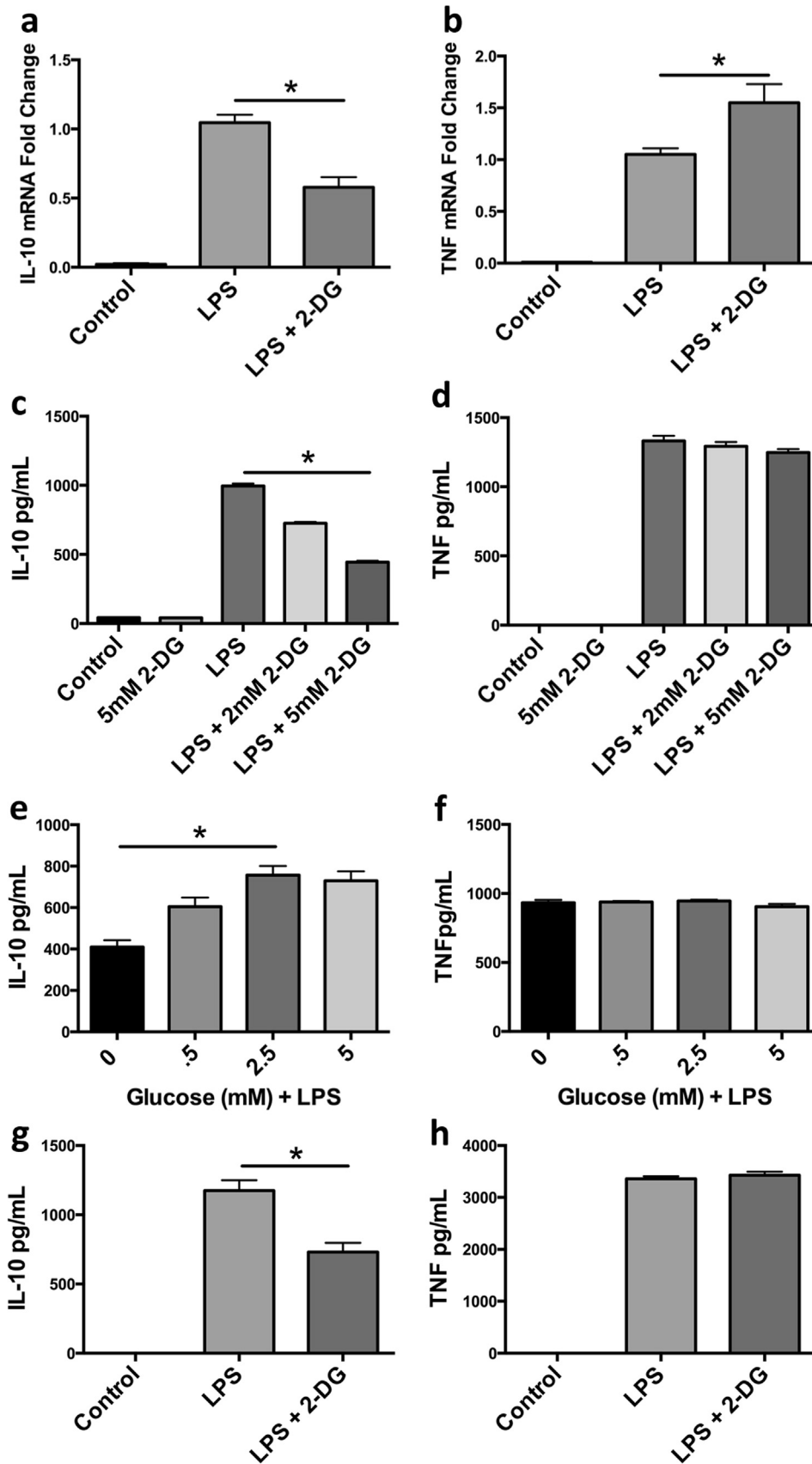


Fig. 3. Inhibition of glycolysis in LPS treated macrophages leads to a reduction in IL-10 but not TNF α . IL-10 and TNF α mRNA (a, b) and protein content (c, d) was measured in BMDM \pm pretreatment of 2-DG (2 mM, 5 mM) followed by stimulation of LPS (100 ng/mL) for 4–5 h. IL-10 and TNF α (e, f) protein content was measured in LPS (100 ng/mL) stimulated BMDM incubated in titrating amount of glucose for 5 h. Human MDM IL-10 and TNF α (g, h) protein content was assessed 5 h post LPS and/or 2-DG pre-treatment. Data are a combination of 3 (a, b) independent experiments or a representative of at least 2 (e, f) or 3 (c, d, g, h) independent experiments * $p < 0.05$. Statistical significance was assessed by ANOVA with a Bonferroni post-test. Error bars represent \pm SEM.

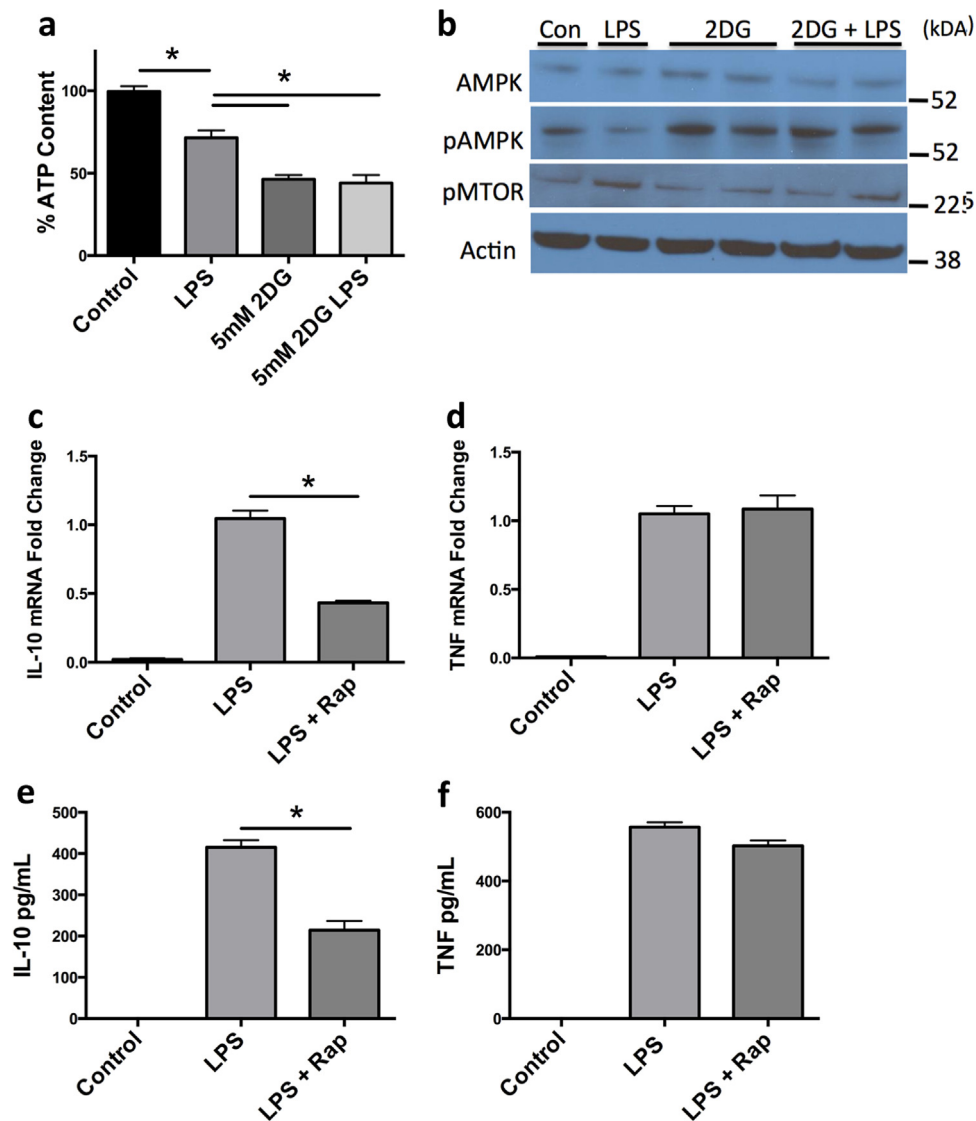


Fig. 4. LPS stimulated IL-10 production in macrophages is controlled via ATP abundance, which acts through AMPK activation and mTOR inhibition. ATP content was measured in BMDM \pm pretreatment of 2-DG (5 mM) for 30 min followed by stimulation of LPS (100 ng/mL) for 4 h (a). BMDM were pretreated with 2-DG \pm LPS and immunoblotted for AMPK, pAMPK, pMTOR, and β -actin (b). IL-10 and TNF α mRNA (c, d) and protein content (e, f) was measured in BMDM \pm pretreatment of Rapamycin (100 nM) followed by stimulation of LPS (100 ng/mL) for 4–5 h. Data are a combination of at least 3 (a, c–d) independent experiments or a representative figure of at least 3 independent experiments (b, e–f) * $p < 0.05$. Statistical significance was assessed by ANOVA with a Bonferroni post-test. Error bars represent \pm SEM.

reductions in IL-10 production (Fig. 4B). Consistent with this mechanism we found that similar to 2-DG, rapamycin potently suppressed LPS-induced IL-10 at mRNA and protein levels without affecting TNF α , confirming mTOR signaling as a key component in LPS-induced IL-10 production (Fig. 4C–F). Taken together, these results suggest a model where LPS stimulation leads to transient reductions in ATP that are not sufficient to activate AMPK allowing mTOR activation to proceed and IL-10 production to occur. However, in the presence of 2-DG, glycolysis is suppressed and ATP levels fall sufficiently low to activate AMPK, suppressing mTOR and blocking IL-10 production.

3.5. Autocrine IL-10 controls both glycolysis and OXPHOS in macrophages

Previous literature has suggested that exogenous IL-10 is capable of repressing LPS-driven glycolysis and inflammatory function in DC [12]. Thus, we hypothesized that because LPS-stimulated macrophages are a substantial source of IL-10, and that IL-10 is regulated by the rate of glycolysis, this cytokine may act in an

autocrine fashion as a rheostat tempering glycolytic commitment. If endogenous LPS-induced IL-10 production is a regulator of metabolic programming, BMDM lacking IL-10 should exhibit a greater degree of metabolic commitment. To test this possibility, we generated BMDM from mice lacking *Il10*. ECAR rates of *Il10*^{-/-} BMDM stimulated with LPS overnight were significantly higher when compared to LPS stimulated wild type (WT) BMDM confirming that autocrine IL-10 production participates in glycolytic regulation (Fig. 5A). Furthermore, OCRs of *Il10*^{-/-} BMDM stimulated overnight with LPS were significantly repressed when compared to LPS stimulated WT BMDM suggesting that autocrine IL-10 might regulate both arms of glycolytic commitment (Fig. 5B). Accordingly, the OCR/ECAR ratio of *Il10*^{-/-} BMDM stimulated overnight with LPS was significantly reduced compared to LPS stimulated WT BMDM indicating an enhanced glycolytic commitment in *Il10*^{-/-} BMDM (Fig. 5C).

The mechanism for OCR suppression in LPS-stimulated macrophages remains unclear. Everts et al. have shown endogenous NO is responsible for the suppression of OCR in DC [11]. Therefore, we stimulated BMDM under conditions we anticipated would

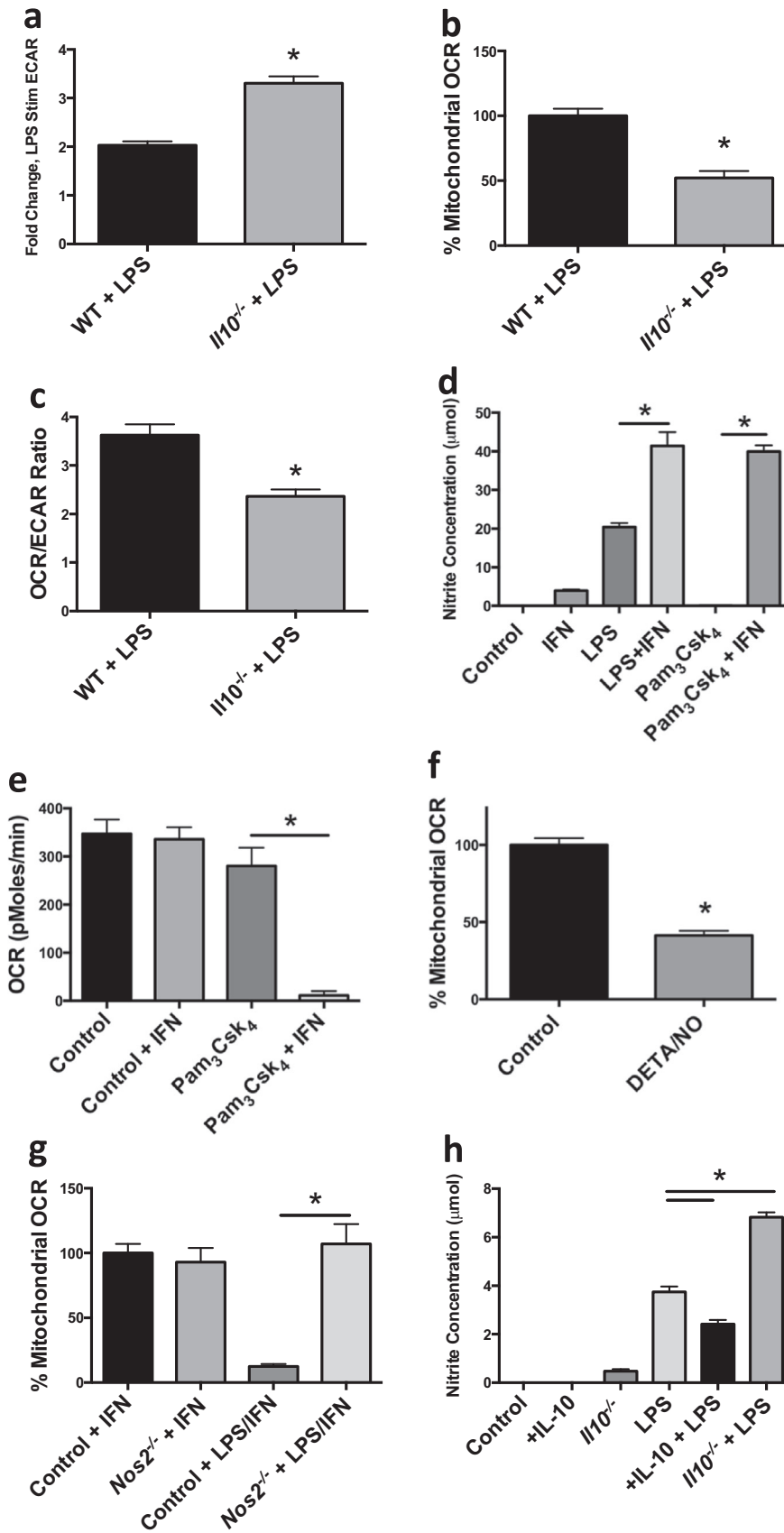


Fig. 5. IL-10 control of macrophage metabolism is via regulation of NO. Metabolic analyses were performed on WT and Il10^{-/-} BMDM 24 h after LPS (100 ng/mL) stimulation including ECAR fold change of LPS treated BMDM compared to non-LPS treated BMDM (a), percent mitochondrial OCR (b), and OCR/ECAR ratio (c). BMDM were treated with for 24 h ± IFN γ (50 ng/mL), ± LPS (100 ng/mL), ± Pam3Csk4 (100 ng/mL) in which nitrite concentrations (d) and OCR (e) were measured. Percent mitochondrial OCR was measured after the addition of NO donor DETA/NO (1 mM) (f). WT and Nos2^{-/-} BMDM mitochondrial OCR were measured after 24 h treatment of IFN γ ± LPS (g). Nitrite concentrations were evaluated in WT and IL-10^{-/-} BMDM 24 h post treatment ± IL-10 (50 ng/mL), ± LPS (h). Metabolic data (a–c, e–g) are representative of 2 independent experiments (mean ± SEM, n=5) *p < 0.05. Figs. d and h are representative figures from 3 independent experiments *p < 0.05. Statistical significance for a–d, f–h were assessed by Student's *t* test. Statistical significance for e and g were assessed by ANOVA with a Bonferroni post-test. Error bars represent ± SEM.

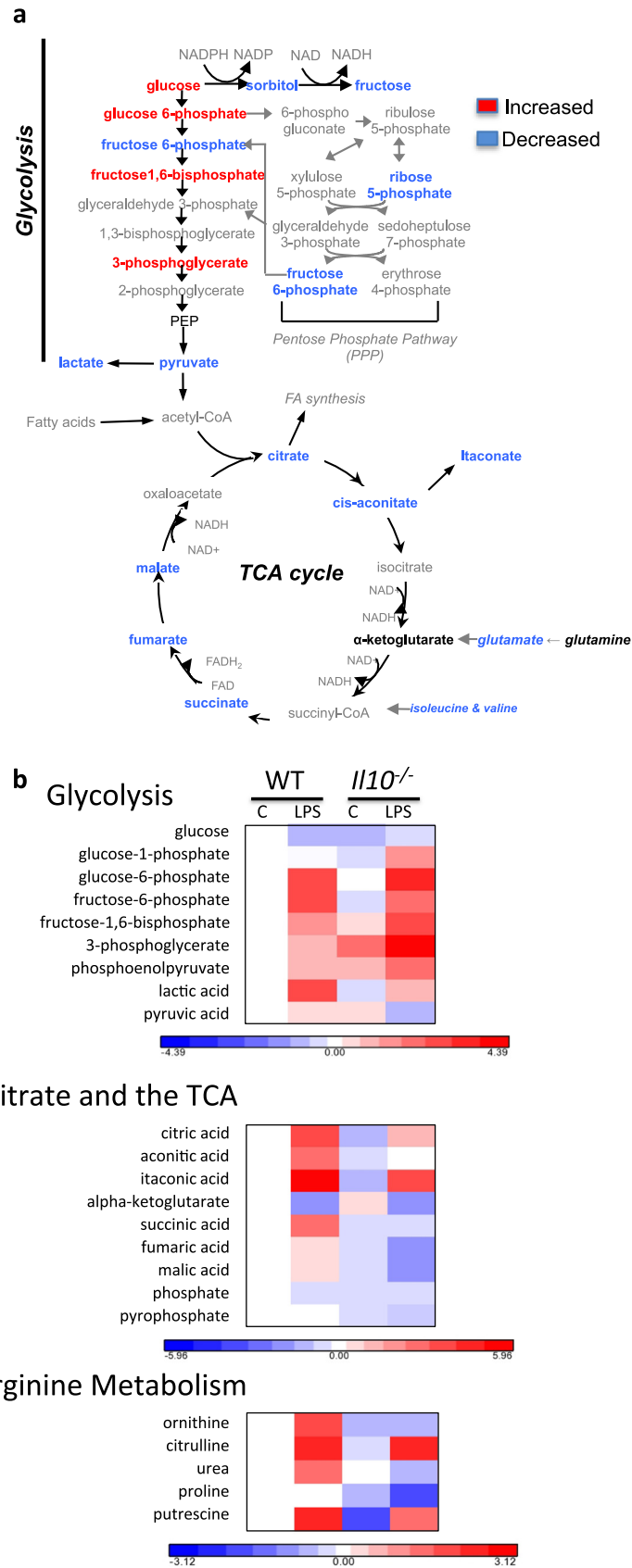


Fig. 6. Primary metabolomic analyses reveal broad scale alterations to glycolytic and TCA cycle metabolites in *Il10^{-/-}* M1 macrophages. WT and *Il10^{-/-}* BMDM were incubated for 24 h in 100 ng/mL LPS prior to GC-TOF analyses. Schematics shown summarize the fold change differences when comparing LPS stimulated *Il10^{-/-}* vs LPS stimulated WT macrophages (a). Colors indicate upregulation (red), downregulation (blue), unchanged (black), or undefined (grey) metabolites. All red or blue colors are statistically significant (p-value < 0.05 and fold change > 10%) except for glucose 6-phosphate (p-value < 0.055, a). (For interpretation of the references to color in this figure legend, the reader is referred to the web version of this article.)

yield various levels of NO production and assayed OXPHOS. As shown in Fig. 5d, stimulation with LPS under conditions that drive glycolytic commitment (Fig. 2) elicited substantial nitrite accumulation in the media, indicative of NO production. In contrast, stimulation with the TLR1/2 agonist Pam₃CSK₄ failed to induce NO production. Co-stimulation with interferon gamma (IFN γ) promoted large amounts of nitrite production in combination with either LPS or Pam₃CSK₄. Therefore, we tested the effects of Pam₃CSK₄ and IFN γ on macrophage OCR. Consistent with the nitrite induction, Pam₃CSK₄ failed to suppress macrophage OCR unless it was combined with IFN γ (Fig. 5E). These data suggest that Toll receptor-mediated glycolytic commitment is dependent on the production of NO.

To directly test the effects of NO on macrophage OXPHOS we tested the effects of direct application of NO. Concentrations of the NO donor DETA/NO that provide concentrations of NO similar to those obtained by LPS and IFN γ -stimulated macrophages led to significant repression of OXPHOS in BMDM (Fig. 5F). Conversely, after culture in LPS, BMDM from *Nos2*^{-/-} mice had significantly higher OCRs than WT cells indicating NO is necessary and sufficient for OXPHOS repression in macrophages (Fig. 5G). Based on these data, we hypothesized that modulation of IL-10 would alter levels of NO in LPS-treated BMDM explaining the effects of endogenous IL-10 on OXPHOS. Indeed, LPS-stimulated BMDM incubated with IL-10 overnight displayed decreased NO production when compared with LPS stimulation alone (Fig. 5H). Conversely, NO levels were significantly higher in LPS treated *Il10*^{-/-} BMDM (Fig. 5H). These data indicate that autocrine IL-10 regulates LPS-induced NO production in BMDM, which in turn is capable of controlling OXPHOS.

Recently, broad scale metabolomic studies on LPS-treated BMDM have shed light on metabolite fluxuations that underlies the phenotypic manifestations associated with glycolytic commitment [4]. Indeed, we also show global metabolic shifts in LPS-treated BMDM including upregulation of glycolytic metabolites (6/7 assayed) (Fig. S2). In addition, LPS-treated BMDM have higher citrate, cis-aconitate and itaconic acid levels; known markers of M1 macrophage polarization [17]. Because our data suggest that both IL-10 and NO play major roles in glycolytic commitment of M1 macrophages, we performed unbiased metabolomic studies on WT, and *Il10*^{-/-} BMDM cultured with or without LPS for 24 h (Fig. 6). In agreement with our metabolic flux data, LPS stimulated *Il10*^{-/-} BMDM had elevated levels of glycolytic metabolites (4/7 assayed) and more pronounced suppression of TCA metabolites (5/6 assayed) when compared to LPS treated WT BMDM (Fig. 6). Notably, the LPS-induced increase in succinate in WT cells was abolished in macrophages lacking IL-10 yet the reductions of alpha-ketoglutarate, indicative of the LPS-induced “TCA break”, is completely intact. This suggests the effects of IL-10 on metabolism are downstream of the break and that they may impact Hif-1 α activation by restraining succinate levels. LPS treated *Il10*^{-/-} BMDM also had decreased pyruvate and lactate levels consistent with their enhanced *Ldha* expression (Fig. 2D), and elevated ECAR (Fig. 6).

As might be expected, we found that LPS treated BMDM accumulate citrulline as a result of the conversion of arginine during the production of NO. Consistent with the high production of NO in macrophages lacking IL-10 these cells had high citrulline levels and were depleted of ornithine, an alternative destination for arginine. Similarly, proline levels declined in stimulated *Il10*^{-/-} macrophages and overall levels of putrescine were lower in these cells consistent with depletion of cellular arginine levels. Taken together these data highlight the substantial effects of IL-10 on M1 metabolic programming.

4. Discussion

Macrophages are immune sentinels that serve as a critical first line of defense during infection [1]. In recent years, it has been shown that stimulation of leukocytes leads to profound metabolic changes that have the ability to alter cellular activation, differentiation, proliferation, and immune functionality [3,18]. During M1 polarization, prolonged LPS stimulation elicits a metabolic commitment towards aerobic glycolysis with strong counter inhibition of mitochondrial OXPHOS [4,6]. Though this metabolic phenomenon has been documented within macrophages, the underlying mechanisms associated with the regulation of glycolytic commitment during polarization remain poorly defined.

IL-10 is highly regulated in macrophages. Co-stimulation of macrophages with immune complexes induces IL-10 via a mechanism involving the re-configuration of the *Il10* locus in a MAPK-dependent manner [19]. Similarly, co-engagement of the immunosuppressive receptor, triggering receptor expressed on myeloid cells- (TREM)-2, promotes IL-10 secretion [15]. Ligands that elicit strong phosphoinositide-3 kinase (PI3K) activation are associated with IL-10 production and via this pathway mTOR has been revealed as key regulator [20–22]. Our findings are consistent with mTOR-driven IL-10 as we find that 2-DG induced ATP starvation enhanced phospho-AMP Kinase, inhibited mTOR and reduced IL-10 production. Accordingly, it has been shown that LPS stimulation of DC leads initially to suppression pAMPK. We believe this also occurs in macrophages, facilitating a burst in IL-10 production, likely through a mechanism involving mTOR activation [12]. Our data show, however, that the very low ATP levels resulting from disruption of glycolysis overwhelm the LPS-driven suppression of pAMPK, leading to diminished IL-10 production. In addition, this finding suggests that although resting macrophages have substantial levels of OXPHOS they are heavily dependent on glycolytic flux to maintain cellular energy levels.

The persistence of substantial OXPHOS over the first several hours of LPS stimulation, in conjunction with the profound suppression seen after 24 h of polarization, suggested that in macrophages repression of OXPHOS might be transcriptional. NO is a known inhibitor of the mitochondrial ETC via reversible inhibition of cytochrome c oxidase and the covalent modification of thiols in Complex I [23,24]. NO is strongly induced during LPS stimulation and we find it to be both necessary and sufficient for the OXPHOS repression evident in M1 macrophages. M1 macrophages derived from mice lacking *Nos2* do not display reduced OXPHOS. In addition, direct application of an NO donor potently suppresses macrophage OXPHOS. Although our finding that NO is responsible for the suppression of OXPHOS associated with glycolytic commitment of macrophages is consistent with reports in DC, it is incongruent with previous studies suggesting that upregulation of pyruvate decarboxylase kinase (PDK)-1, an inhibitor of acetyl-CoA synthesis, may be responsible for OXPHOS regulation in macrophages [9]. Yang et al. found that of HIF-1 α transcriptional activity, an effect reportedly associated with succinate accumulation in M1 macrophages, can promote PDK1 mRNA accumulation in both BMDM and RAW264.7 cells. However, such a model of PDK-1-mediated suppression of OXPHOS, although demonstrated in tumor cells, is inconsistent with the known need for substantial citrate export from the mitochondria during proinflammatory cytokine production. In DC, citrate exported from the mitochondria facilitates production of fatty acids needed for endoplasmic reticulum expansion and development of the Golgi apparatus required for cytokine production [5]. Suppression of pyruvate dehydrogenase by induced PDK-1 would be expected to deprive the citrate carrier of glucose-derived cargo and blunt these pro-inflammatory functions. Furthermore, our finding of accelerated rates of glycolysis in *Il10*^{-/-} M1 macrophages where succinate has

not accumulated argue against a role for a succinate-HIF1 α -PDK-1 mechanism in the M1 metabolic polarization. Therefore, although it is clear that HIF-1 α does play a role in glycolytic enhancement, as appreciated as increased expression of multiple HIF-1 α targets in LPS stimulated BMDM, we propose that the down-regulation of OXPHOS during commitment is mediated entirely via NO and independent of Hif1 α -driven PDK-1 expression. Consistent with this model, NO is known to facilitate the stabilization of Hif1 α via direct suppression of the proyl-hydroxylases (PHD) [25]. However, the dependency of LPS-induced, Hif1 α -driven transcription on NO production is unclear and requires further study.

M1 polarization of BMDM leads to profound metabolic changes including alterations to the glycolytic pathway and TCA cycle. Our metabolomics data from LPS stimulated BMDM are in general agreement with the broken TCA cycle hypothesis in which the TCA cycle is blocked, allowing the build up and cytosolic export of citrate and subsequent itaconic acid production. In addition we also find evidence that the arginosuccinate pathway is elevated, permitting accelerated production of NO. Jha et al. suggests that suppression of isocitrate dehydrogenase (*Idh1*), which converts isocitrate to α -ketoglutarate, is the critical factor for TCA rerouting in M1 macrophages [26]. Our metabolomics show that citrate accumulation, albeit somewhat truncated, occurs in cells lacking IL-10 while these cells also show a substantial reduction in alpha ketoglutarate. Together these findings show that the TCA break is intact in *IL10*^{-/-} M1 macrophages. In fact, we find the levels of TCA intermediates to be even lower in M1 macrophages lacking IL-10 than in WT cells.

The data we present here suggests that a component of the anti-inflammatory effects of IL-10 may lie with its ability to regulate the metabolic program of myeloid cells. Previous reports have suggested that IL-10 can suppress the expression of a glycolytic phenotype in DC but our findings demonstrate an alternative mode of action [12]. By suppressing the production of NO, autologous IL-10 preserves OXPHOS in macrophages. Thus the cytokine affects both aspects of metabolic programming strongly favoring a phenotype high in OXPHOS. Our finding that IL-10 production is itself subject to regulation by glucose availability during transition to glycolysis demonstrates its role as a rheostat controlling commitment in macrophages. Disruption of this rheostat in *Il10* null mice results in substantially increased NO production, increased glycolytic flux, and further suppressed OXPHOS.

Though multiple studies have identified IL-10 as a potent regulator of NO production, the mechanisms behind this phenomenon remain unclear. Some reports suggest that IL-10 acts at the transcriptional level via inhibition of *Nos2* expression whereas others show enhanced degradation of NO [27,28]. Alternatively, IL-10 is reported to block iNOS accumulation without affecting *Nos2* mRNA, to induce competing arginase activity, or to suppress LPS-mediated up regulation of the type-2 cationic amino acid transporter (CAT2) that facilitates arginine uptake [29]. Our data suggest that regardless of its mode of action, the repression of NO and the associated maintenance of oxidative respiration by IL-10 promotes the highly oxidative program.

In summary, we have shown that acute LPS stimulation of macrophages leads to an immediate enhancement of glycolysis followed by long term repression of mitochondrial OXPHOS. Further, we have found that this mechanism of glycolytic commitment is NO and IL-10 dependent. Specifically, we propose that IL-10 acts as a metabolic rheostat capable of fine-tuning the glycolytic commitment. This is evident during macrophage stimulation and occurs via regulation of NO production, which exerts pronounced effects at a variety of points within cellular metabolism. Through continued efforts aimed at elucidating mechanisms, such as this, that balance between pathogenicity, immunity and

metabolism, we hope to unearth attractive new metabolic targets that can aid in the regulation of inflammatory response.

Appendix A. Supporting information

Supplementary data associated with this article can be found in the online version at <http://dx.doi.org/10.1016/j.redox.2016.09.005>.

References

- [1] O. Soehnlein, L. Lindbom, Phagocyte partnership during the onset and resolution of inflammation, *Nat. Rev. Immunol.* 10 (2010) 427–439.
- [2] L.C. Davies, P.R. Taylor, Tissue-resident macrophages: then and now, *Immunology* 144 (2015) 541–548.
- [3] K. Ganeshan, A. Chawla, Metabolic regulation of immune responses, *Annu. Rev. Immunol.* 32 (2014) 609–634.
- [4] G.M. Tannahill, A.M. Curtis, J. Adamik, E.M. Palsson-McDermott, A. F. McGettrick, G. Goel, C. Frezza, N.J. Bernard, B. Kelly, N.H. Foley, L. Zheng, A. Gardet, Z. Tong, S.S. Jany, S.C. Corr, M. Haneklaus, B.E. Caffrey, K. Pierce, S. Walmsley, F.C. Beasley, E. Cummins, V. Nizet, M. Whyte, C.T. Taylor, H. Lin, S. L. Masters, E. Gottlieb, V.P. Kelly, C. Clish, P.E. Auron, R.J. Xavier, L.A. O'Neill, Succinate is an inflammatory signal that induces IL-1 β through HIF-1 α , *Nature* 496 (2013) 238–242.
- [5] B. Everts, E. Amiel, S.C. Huang, A.M. Smith, C.H. Chang, W.Y. Lam, V. Redmann, T.C. Freitas, J. Blagih, G.J. van der Windt, M.N. Artyomov, R.G. Jones, E.L. Pearce, E.J. Pearce, TLR-driven early glycolytic reprogramming via the kinases TBK1-IKK ν epsilon supports the anabolic demands of dendritic cell activation, *Nat. Immunol.* 15 (2014) 323–332.
- [6] J.C. Rodriguez-Prados, P.G. Traves, J. Cuenca, D. Rico, J. Aragones, P. Martin-Sanz, M. Cascante, L. Bosca, Substrate fate in activated macrophages: a comparison between innate, classic, and alternative activation, *J. Immunol.* 185 (2010) 605–614.
- [7] D. Vats, L. Mukundan, J.I. Odegaard, L. Zhang, K.L. Smith, C.R. Morel, R. A. Wagner, D.R. Greaves, P.J. Murray, A. Chawla, Oxidative metabolism and PGC-1 β attenuate macrophage-mediated inflammation, *Cell Metab.* 4 (2006) 13–24.
- [8] S.C. Huang, B. Everts, Y. Ivanova, D. O'Sullivan, M. Nascimento, A.M. Smith, W. Beatty, L. Love-Gregory, W.Y. Lam, C.M. O'Neill, C. Yan, H. Du, N.A. Abumrad, J.F. Urban Jr., M.N. Artyomov, E.L. Pearce, E.J. Pearce, Cell-intrinsic lysosomal lipolysis is essential for alternative activation of macrophages, *Nat. Immunol.* 15 (2014) 846–855.
- [9] L. Yang, M. Xie, M. Yang, Y. Yu, S. Zhu, W. Hou, R. Kang, M.T. Lotze, T.R. Billiar, H. Wang, L. Cao, D. Tang, PKM2 regulates the Warburg effect and promotes HMGB1 release in sepsis, *Nat. Commun.* 5 (2014) 4436.
- [10] J.W. Kim, I. Tchernyshyov, G.L. Semenza, C.V. Dang, HIF-1-mediated expression of pyruvate dehydrogenase kinase: a metabolic switch required for cellular adaptation to hypoxia, *Cell Metab.* 3 (2006) 177–185.
- [11] B. Everts, E. Amiel, G.J. van der Windt, T.C. Freitas, R. Chott, K.E. Yarasheski, E. L. Pearce, E.J. Pearce, Commitment to glycolysis sustains survival of NO-producing inflammatory dendritic cells, *Blood* 120 (2012) 1422–1431.
- [12] C.M. Krawczyk, T. Holowka, J. Sun, J. Blagih, E. Amiel, R.J. DeBerardinis, J. R. Cross, E. Jung, C.B. Thompson, R.G. Jones, E.J. Pearce, Toll-like receptor-induced changes in glycolytic metabolism regulate dendritic cell activation, *Blood* 115 (2010) 4742–4749.
- [13] I.R. Turnbull, S. Gilfillan, M. Cella, T. Aoshi, M. Miller, L. Piccio, M. Hernandez, M. Colonna, Cutting edge: TREM-2 attenuates macrophage activation, *J. Immunol.* 177 (2006) 3520–3524.
- [14] S.K. Sen, K.C. Boelte, J.J. Barb, R. Joehanes, X. Zhao, Q. Cheng, L. Adams, J.K. Teer, D.S. Accame, S. Chowdhury, L.N. Singh, M. Kavousi, P.A. Peyser, L. Quigley, D. L. Priel, K. Lau, D.B. Kuhns, T. Yoshimura, A.D. Johnson, S.J. Hwang, M.Y. Chen, A.E. Arai, E.D. Green, J.C. Mullikin, F.D. Koldogly, C.J. O'Donnell, R. Virmani, P. J. Munson, D.W. McVicar, L.G. Biesecker, Integrative DNA, RNA, and protein evidence connects TREML4 to coronary artery calcification, *Am. J. Hum. Genet.* 95 (2014) 66–76.
- [15] G.C. Whittaker, S.J. Orr, L. Quigley, L. Hughes, I.M. Francischetti, W. Zhang, D. W. McVicar, The linker for activation of B cells (LAB)/non-T cell activation linker (NTAL) regulates triggering receptor expressed on myeloid cells (TREM)-2 signaling and macrophage inflammatory responses independently of the linker for activation of T cells, *J. Biol. Chem.* 285 (2010) 2976–2985.
- [16] D.G. Hardie, F.A. Ross, S.A. Hawley, AMPK: a nutrient and energy sensor that maintains energy homeostasis, *Nat. Rev. Mol. Cell Biol.* 13 (2012) 251–262.
- [17] C.L. Strelko, W. Lu, F.J. Dufort, T.N. Seyfried, T.C. Chiles, J.D. Rabinowitz, M. F. Roberts, Itaconic acid is a mammalian metabolite induced during macrophage activation, *J. Am. Chem. Soc.* 133 (2011) 16386–16389.
- [18] N.J. MacIver, R.D. Michalek, J.C. Rathmell, Metabolic regulation of T lymphocytes, *Annu. Rev. Immunol.* 31 (2013) 259–283.
- [19] M. Lucas, X. Zhang, V. Prasanna, D.M. Mosser, ERK activation following macrophage Fc γ 3R ligation leads to chromatin modifications at the IL-10 locus, *J. Immunol.* 175 (2005) 469–477.
- [20] T. Fukao, M. Tanabe, Y. Terauchi, T. Ota, S. Matsuda, T. Asano, T. Kadowaki,

- T. Takeuchi, S. Koyasu, PI3K-mediated negative feedback regulation of IL-12 production in DCs, *Nat. Immunol.* 3 (2002) 875–881.
- [21] M. Saraiva, A. O'Garra, The regulation of IL-10 production by immune cells, *Nat. Rev. Immunol.* 10 (2010) 170–181.
- [22] T. Weichhart, G. Costantino, M. Poglitsch, M. Rosner, M. Zeyda, K. M. Stuhlmeier, T. Kolbe, T.M. Stulnig, W.H. Horl, M. Hengstschlager, M. Muller, M.D. Saemann, The TSC-mTOR signaling pathway regulates the innate inflammatory response, *Immunity* 29 (2008) 565–577.
- [23] M.W. Cleeter, J.M. Cooper, V.M. Darley-Usmar, S. Moncada, A.H. Schapira, Reversible inhibition of cytochrome c oxidase, the terminal enzyme of the mitochondrial respiratory chain, by nitric oxide. Implications for neurodegenerative diseases, *FEBS Lett.* 345 (1994) 50–54.
- [24] E. Clementi, G.C. Brown, M. Feelisch, S. Moncada, Persistent inhibition of cell respiration by nitric oxide: crucial role of S-nitrosylation of mitochondrial complex I and protective action of glutathione, *Proc. Natl. Acad. Sci. USA* 95 (1998) 7631–7636.
- [25] E. Metzzen, J. Zhou, W. Jelkmann, J. Fandrey, B. Brune, Nitric oxide impairs normoxic degradation of HIF-1 α by inhibition of prolyl hydroxylases, *Mol. Biol. Cell* 14 (2003) 3470–3481.
- [26] A.K. Jha, S.C. Huang, A. Sergushichev, V. Lampropoulou, Y. Ivanova, E. Loginicheva, K. Chmielewski, K.M. Stewart, J. Ashall, B. Everts, E.J. Pearce, E. M. Driggers, M.N. Artyomov, Network integration of parallel metabolic and transcriptional data reveals metabolic modules that regulate macrophage polarization, *Immunity* 42 (2015) 419–430.
- [27] F.Q. Cunha, S. Moncada, F.Y. Liew, Interleukin-10 (IL-10) inhibits the induction of nitric oxide synthase by interferon-gamma in murine macrophages, *Biochem. Biophys. Res. Commun.* 182 (1992) 1155–1159.
- [28] W.C. Huang, Y.S. Lin, C.Y. Wang, C.C. Tsai, H.C. Tseng, C.L. Chen, P.J. Lu, P.S. Chen, L. Qian, J.S. Hong, C.F. Lin, Glycogen synthase kinase-3 negatively regulates anti-inflammatory interleukin-10 for lipopolysaccharide-induced iNOS/NO biosynthesis and RANTES production in microglial cells, *Immunology* 128 (2009) e275–e286.
- [29] C.J. Huang, B.R. Stevens, R.B. Nielsen, P.N. Slovin, X. Fang, D.R. Nelson, J. W. Skimming, Interleukin-10 inhibition of nitric oxide biosynthesis involves suppression of CAT-2 transcription, *Nitric Oxide* 6 (2002) 79–84.